Title

Hybrid silicon evanescent laser fabricated with a silicon waveguide and III-V offset quantum well

Permalink

https://escholarship.org/uc/item/76j4d9wz

Journal

Optics Express, 13(23)

ISSN

1094-4087

Authors

Park, H
Fang, A W
Kodama, S
et al.

Publication Date

2005-11-01

Peer reviewed

A hybrid silicon evanescent laser fabricated with a silicon waveguide and III-V offset quantum wells

Hyundai Park, Alexander W. Fang, Satoshi Kodama[a], and John E. Bowers

University of California Santa Barbara, ECE Department
Santa Barbara, CA 93106-9560, USA
hdpark@engr.ucsb.edu

Abstract: A novel laser that utilizes a silicon waveguide bonded to AlGaInAs quantum wells is demonstrated. This wafer scale fabrication approach allows the optical waveguide to be defined by CMOS-compatible silicon processing while optical gain is provided by III-V materials. The AlGaInAs quantum well structure is bonded to the silicon wafer using low temperature oxygen plasma-assisted wafer bonding. The optically pumped 1538 nm laser has a pulsed threshold of 30 mW and an output power of 1.4 mW.

OCIS codes: (140.5960) Semiconductor lasers; (250.5300) Photonic integrated circuits.

References and links

1. G.T. Reed and A. P. Knights, Silicon Photonics: An Introduction (John Wiley, Chichester, UK, 2004).
2. A. Liu, R. Jones, L. Liao, D. Samara-Rubio, D. Rubin, O. Cohen, R. Nicolaescu, and M. Paniccia, "A high-speed silicon optical modulator based on a metal-oxide-semiconductor capacitor," Nature **427**, 615-618 (2004).
3. B. Jalali, S. Yegnanarayanan, T. Yoon, T. Yoshimoto, I. Rendina, and F. Coppinger, "Advances in Silicon-on-Insulator Optoelectronics," IEEE J. Sel. Topics Quantum Electron. **4**, 938-947 (1998).
4. H. Rong, R. Jones, A. Liu, O. Cohen, D. Hak, A. Fang and M. Paniccia, "A continuous-wave Raman silicon laser," Nature **433**, 725-728 (2005).
5. O. Boyraz, and B. Jalali, "Demonstration of a silicon Raman laser," Opt. Express **12**, 5269-5273 (2004).
6. B. Gelloz and N. Koshida, "Electroluminescence with high and stable quantum efficiency and low threshold voltage from anodically oxidized thin porous silicon diode," J. Appl. Phys. **88**, 4319-4324 (2000).
7. A. Irrera, D. Pacifici, M. Miritello, G. Franzo, F. Priolo, F. Iacona, D. Sanfilippo, G. Di Stefano, and P.G. Fallica, "Electroluminescence properties of light emitting devices based on silicon nanocrystals," Physica E **16**, 395-399 (2003).
8. G. Dehlinger, L. Diehl, U. Gennser, H. Sigg, J. Faist, K. Ensslin, D. Grützmacher, and E. Müller, "Intersubband Electroluminescence from Silicon-Based Quantum Cascade Structures," Science **290**, 2277-2280 (2000).
9. W. L. Ng, M. A. Lorenco, R. M. Gwilliam, S. Ledain, G. Shao, and K. P. Homewood, "An efficient room-temperature silicon-based light-emitting diode," Nature **410**, 192-194 (2001).
10. G. Franzò, S. Coffa, F. Priolo, and C. Spinella, "Mechanism and performance of forward and reverse bias electroluminescence at 1.54 μm from Er-doped Si diodes," J. Appl. Phys. **81**, 2784-2793 (1997).
11. H. Wada and T. Kamijoh, "Room-Temperature CW operation of InGaAsP Lasers on Si Fabricated by Wafer Bonding," IEEE Photon. Technol. Lett. **8**, 173-175 (1996).
12. M. Razeghi, M. Defour, R. Blondeau, F. Omnes, P. Maurel, O. Acher, F. Brillouet, J. C. C-Fan and J. Salerno, "First cw operation of a $Ga_{0.25}In_{0.75}As_{0.5}P_{0.5}$-InP laser on a silicon substrate," Appl. Phys. Lett. **53**, 2389-2390 (1988).
13. A. Karim, K. A. Black, P. Abraham, D. Lofgreen, Y. J. Chiu, J. Piprek, and J. E. Bowers, "Super lattice barrier 1528-nm vertical-cavity laser with 85°C continuous-wave operation," IEEE Photon. Technol. Lett. **12**, 1438-1440 (2000).
14. D. Pasquariello and K. Hjort, "Plasma-Assisted InP-to-Si Low Temperature Wafer Bonding," IEEE J. Sel. Top. Quantum Electron. **8**, 118-131 (2002).

[a] He was a visiting researcher at UCSB. He is now at NTT Photonics Laboratories, NTT Corporation, 3-1 Morinosato Wakamiya, Atsugi-shi, Kanagawa 243-0198, Japan.

1. Introduction

Silicon-based photonic devices are of great interest for the integration of photonic devices with Si VLSI CMOS technology providing improvements in performance, yield, and cost [1]. The focus of this research has been on passive devices such as AWGs and modulators [2, 3], and it is a challenge to build light-emitting devices, because silicon is an indirect bandgap semiconductor. One approach to build optically pumped lasers on a silicon substrate is a Raman laser [4, 5]. LEDs have been built using porous silicon [6], nanocrystalline-Si [7], SiGe quantum cascade structures [8], dislocation-engineered silicon [9] and erbium doped SiO2 [10]. Heterogeneous integration techniques to combine optically active materials with a silicon substrate including wafer bonding [11] and heteroepitaxy [12] are also interesting. A unique approach demonstrated in this paper utilizes a silicon waveguide mode evanescently coupled to III-V multiple quantum wells. This approach combines the advantages of high gain III-V materials and the integration capability of silicon technology. Moreover, the difficulty of coupling to silicon-based passive optical devices is overcome by confining most of the optical mode to the silicon waveguide. We report the first demonstration of a silicon evanescently coupled laser in this paper and report a 1538 nm laser with an optically pumped threshold of 30 mW and a maximum power output of 1.4 mW at 12 ºC. This demonstration raises the possibility of a range of high performance optical devices such as electrically pumped lasers, amplifiers, modulators, and detectors integrated on silicon.

2. Device Structure and Fabrication

The device structure is shown in Fig. 1. The device is divided into two regions: the silicon-on-insulator (SOI) passive-waveguide structure and the III-V active region that provides the optical gain. The SOI structure consists of a Si substrate, a 500 nm-thick SiO_2 lower cladding layer, and a Si rib waveguide with a height (H), width (W) and rib-etch depth (D) of 0.97 μm, 1.3 μm, and 0.78 μm respectively. The III-V region consists of a two-period InP/1.1 μm InGaAsP super lattice (SL), a 110 nm thick InP spacer, a 50 nm thick unstrained 1.3 μm AlGaInAs separated confinement heterostructure (SCH) layer, strain-compensated InAlGaAs quantum wells, a 500 nm thick unstrained 1.3 μm AlGaInAs SCH layer, and an InP upper cladding layer. The SL region employs 7.5 nm thick alternating layers of InP/InGaAsP to inhibit the propagation of defects from the bonded interface to the QW region [13]. Five 70 nm thick AlGaInAs quantum wells with compressive strain (0.85 %) and 100 nm-thick AlGaInAs barriers with tensile strain (-0.55 %) are used. The barrier layers have a bandgap corresponding to a wavelength of 1.3 μm. The resulting hybrid structure supports a fundamental transverse mode with a Si waveguide transverse confinement factor, Γ_{Si}, of 42.8 % and a QW transverse confinement factor, Γ_{QW}, of 3.6 % for five quantum wells.
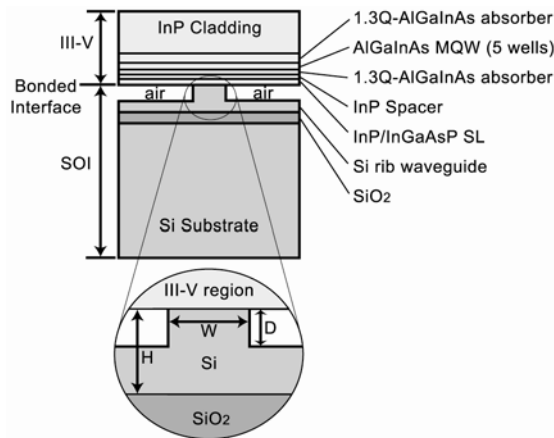

Fig. 1. Cross-section device structure of an SOI rib waveguide bonded to a III-V active region epitaxial structure.

The SOI structure is processed by forming an SiO_2 mask layer through thermal oxidation for 2 hours at 1050 °C on an undoped (100) SOI wafer. The silicon rib waveguides are then formed using inductively coupled plasma (ICP) etching with Cl_2/BCl_3. The SOI wafer and III-V epitaxial wafer are treated by buffered HF and NH_4OH respectively after a thorough cleaning procedure using acetone, isopropanol, and deionized water. The two samples are bonded together via oxygen plasma assisted wafer bonding [14]. After a low temperature anneal (~250 °C), the InP substrate is removed with HCl. Finally, the devices are diced and the facets are polished and coated with a broadband dielectric HR coating (~80 %) consisting of three periods of SiO_2/Ta_2O_5. The final device length after dicing and polishing is 600 μm. A scanning electron microscope (SEM) cross-section image of the structure is shown in Fig. 2.

The optical gain of quantum wells is preserved by the low temperature annealing process. The large mismatch in thermal expansion coefficients between Si (2.6 x 10^{-6} K^{-1}) and InP (4.8 x 10^{-6} K^{-1}) can introduce dislocations or cracks at temperatures above 300 °C for the substrate thicknesses of 500 μm and 350 μm for Si and InP respectively. Annealed devices at 600 °C without plasma treatment commonly show surface non-uniformities when observed though a microscope after InP substrate removal. Moreover, the high temperature bonding process results in a reduction of photoluminescence intensity by a factor of six relative to low-temperature oxygen plasma assisted bonding.

The oxygen plasma treatment generates an ultra thin oxide layer (<5 nm) whose surface is very smooth and highly chemically reactive [14]. As a result, this bonding process creates a thin oxide layer at the bonded interface, which does not significantly alter the optical mode because it is so thin and optically transparent.
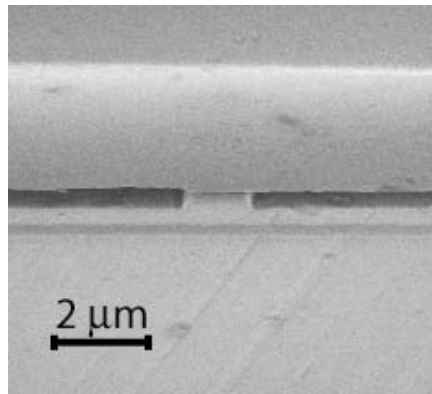

Fig. 2. SEM cross section of the fabricated device before HR coating.

3. Experiment and Results

The device is optically pumped perpendicular to the laser by a 980 nm laser diode. The light from a pump laser diode is focused by a cylindrical lens illuminating a 10 μm by 916 μm rectangular spot incident on the device through the top InP cladding layer. The pump laser is operated pulsed to increase the pump power. The laser output is collected with a lensed fiber from the waveguide and characterized by a spectrum analyzer or photodetector. The coupling loss of a lensed fiber is experimentally measured to be 5dB. The TE/TM near-field images of the output mode are recorded on an IR camera through a polarizing beam splitter and an 80x lens at the opposite waveguide facet.

Figure 3(a) illustrates the mode profile calculated with BeamPROP using the device dimensions stated above. Figure 3(b) shows a TE near-field image from the laser. As shown in Fig. 3b, the lasing mode is predominantly TE and its mode profile is similar to the calculated

mode depicted in Fig. 3(a). The extinction ratio between TE mode and TM mode is > 20 dB. It is important to note that lasing only occurs in the optical mode defined by the Si waveguide region. In other words, slab modes in the III-V region do not support lasing. This can be seen from the inset of Fig. 4, which compares the light output for pumping in the two regions. This can also be seen by translating the pump beam across the rib waveguide. The optical output power drops with a FWHM of 6 µm wider than the width of the rib, as expected from the finite pump beamwidth of 10 µm.
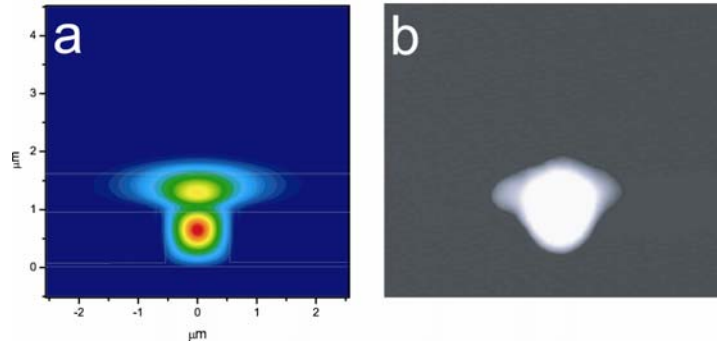

Fig. 3. (a) Calculated TE fundamental mode profile (b) TE near field image of lasing optical mode.

Figure 4 shows the laser output power collected by a lensed fiber through a single facet as a function of average pump power and temperature. The threshold increases from 30 to 50 mW between 12 °C and 20 °C and the structure exhibits a temperature coefficient (T_0) of 18 K. This low T_0 is largely due to the lack of carrier confinement structure in the 0.5 µm thick absorber layer. The maximum output power of 1.4 mW is limited by the pump laser power available, and is not thermally limited. The single output differential quantum efficiency is approximately 3.2 % at 12 ºC, and the total efficiency taking into account the light from both facets and the coupling losses of 5 dB is approximately 20 %.

Figure 5 shows the lasing spectrum at 1.4 times the threshold pump power and at a temperature of 12 ºC. The optical spectrum consists of the expected Fabry-Pérot response for the 600 µm long cavity, with a group index of 3.85. The calculated group index from simulations is 3.81.
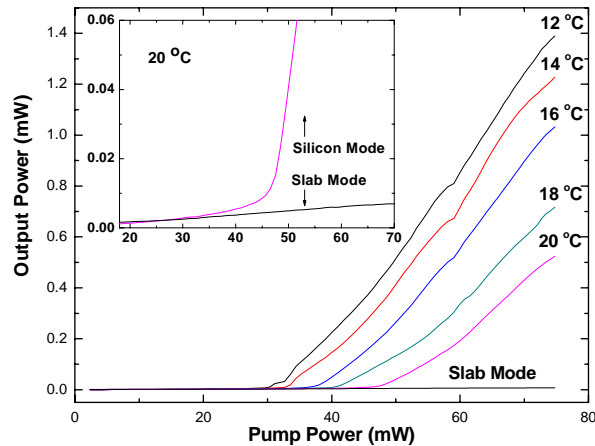

Fig. 4. Single-sided fiber-coupled output power of the silicon evanescent laser as a function of pump power for several temperatures.
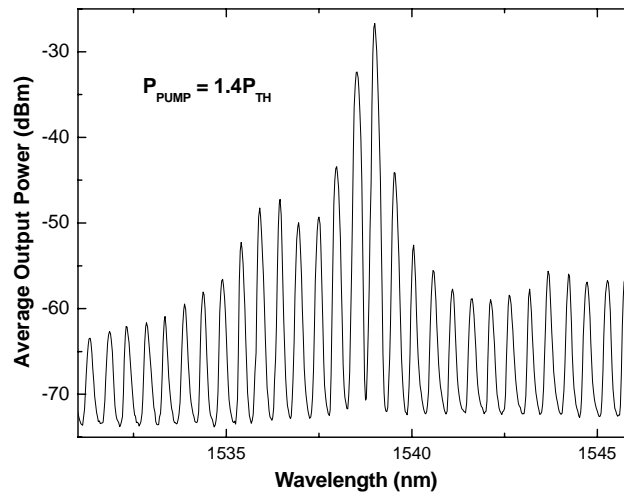
Fig. 5. Spectrum of the silicon evanescent laser operating at 1538 nm. The spectrum is measured at 1.4 times the threshold power at 12 °C with 0.1 nm resolution.

4. Conclusion

An optically pumped silicon evanescent laser consisting of an AlGaInAs/InP active region bonded to a passive silicon waveguide has been successfully demonstrated. The laser has a threshold pump power of 30 mW and a single-sided slope efficiency of 3.2 % operating at 1538 nm. The fabrication procedure includes standard CMOS-compatible processing of the silicon waveguides and a low-temperature oxide-mediated wafer bonding process for heterogeneous integration. The low temperature laser process flow (maximum temperature of 400 °C) allows for back end processing of the optoelectronic elements after the CMOS process has been completed. Moreover, the plasma-activated wafer bonding yields sufficient bonding strength to endure dicing and facet polishing. This work is the first step to integrate high performance active optical circuits with silicon VLSI electronics and can be extended directly into electrically pumped lasers by providing doped layers and patterning mesa structures in III-V region to flow electrical currents through the III-V active region. It is also feasible to build other optically active devices including amplifiers, modulators, and detectors with this approach.